Data, Innovation, and Science Cluster

Swarm-TIRO Description of the Processing Algorithms

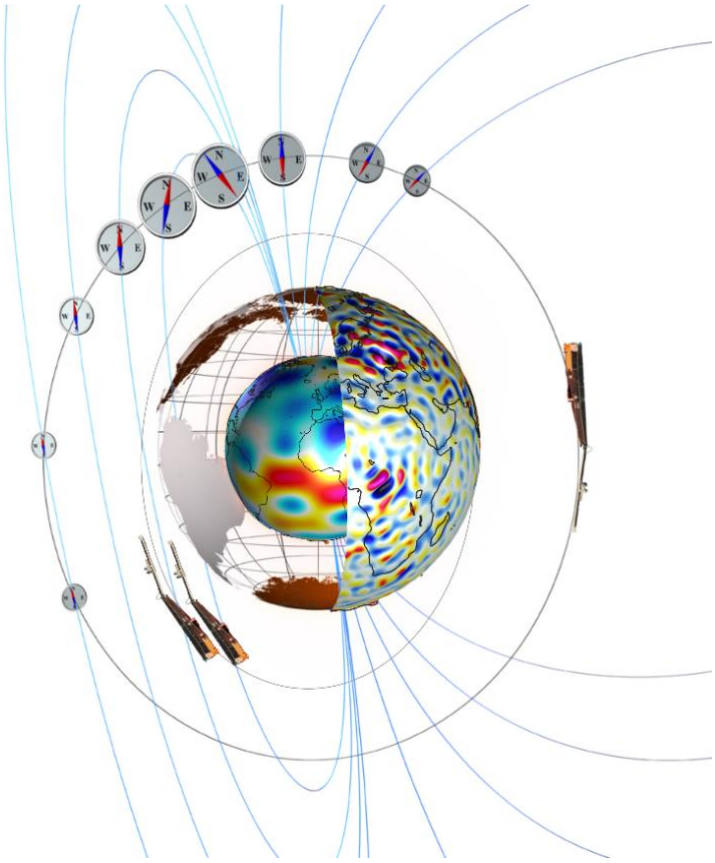

Doc. no: SW-DS-GFZ-GS-012, Rev: 1, 28 Mar 2022

Prepared: Guram Kervalishvili — Digitally signed by Guram Kervalishvili Date: 2022.03.28 23:42:23 +02'00'

Guram Kervalishvili — Date 28 Mar 2022

GFZ Team Leader

Checked:

Lucas Schreiter — Date 28 Mar 2022

Scientist

Approved: Claudia Stolle — Digitally signed by Claudia Stolle Date: 2022.03.29 11:09:56 +02'00'

Claudia Stolle — Date 28 Mar 2022

TIRO Project Leader

Record of Changes

Reason	Description	Rev	Date
Initial vers.	Released.	1 dA	31 May 2021
Email from Nils to Claudia: 03.06.2021, 16h15	Document text has been updated and corrected with major changes.	1 dB	01 Jul 2021
Email from Nils to Claudia: 29.08.2021, 15h57	Document text has been updated and corrected with suggested changes.	1 dC	07 Sep 2021
Updated input from consortium	Document text has been updated and corrected with suggested changes.	1 dD	27 Mar 2022
Signature		1	28 Mar 2022

Table of Contents

List of Figures

1 Introduction

1.1 Scope and applicability

This document comprises the description of the processing algorithms of Swarm-TIRO Level 2 (L2) products in response to the requirements of [AD-1]. Swarm-TIRO includes two groups of products: Total Electron Content (TEC) derived from the dual frequency Global Positioning System (GPS) observations and electron density (Ne) derived from the dual frequency measurements obtained from the inter-satellite K-Band ranging (KBR) system using measurements from the following multi-satellite missions [AD-2]:

- CHAMP – **TEC_TMS_2F**;
- GRACE – **TEC1TMS_2F**, **TEC2TMS_2F**, and **NE__KBR_2F**;
- GRACE-FO – **TEC1TMS_2F**, **TEC2TMS_2F**, and **NE__KBR_2F**.

The Swarm-TIRO Product Definition Document (PDD) [AD-2] describing the product names and content as well as this document are available in the SVN folder: https://smart-svn.spacecenter.dk/svn/smart/SwarmDISC/DISC_Projects/ITT3_3_TIRO/Deliverables/.

2 Applicable and Reference Documentation.

2.1 Applicable Documents

The following documents are applicable to the definitions used within this document.

[AD-1] SW-OF-GFZ-GS-126_3-3_TIRO, Proposal for Swarm DISC ITT 3.3, Swarm-TIRO – Topside Ionosphere Radio Observations from multiple LEO-missions, https://smart-svn.spacecenter.dk/svn/smart/SwarmDISC/DISC_Projects/ITT3_3_TIRO/Proposal/.

[AD-2] TN-01: SW-DS-GFZ-GS-010_3-3_TIRO_PDD, Product Definition Document.

[AD-3] SW-DS-GFZ-GS-0004 (Rev. 4a, 2016), Swarm Level 2 Processing System - GFZ Detailed Processing Model TEC.

[AD-4] GRACE Level 1B Data Product User Handbook (Rev. 1.3, 2010), ftp://isdcftp.gfz-potsdam.de/grace/DOCUMENTS/Level-1/GRACE_L1B_Data_Product_User_Handbook.pdf.

[AD-5] TN-04: SW-DS-GFZ-GS-013_3-3_TIRO_VR, Validation Report.

2.2 Reference Documents

The following documents contain additional information about the methods used and external data sources.

[RD-1] Blewitt, G. (1990), An automated editing algorithm for GPS data, Geophysical Research Letters, 17, 199–202, doi: 10.1029/GL017i003p00199.

[RD-2] Yue, X., Schreiner, W. S., Hunt, D. C., Rocken, C., Kuo, Y.-H. (2011), Quantitative evaluation of the low Earth orbit satellite based slant total electron content determination, Space Weather, 9, S09001, doi: 10.1029/2011SW000687.

[RD-3] Noja, M., Stolle, C., Park, J., Lühr (2013), Long-term analysis of ionospheric polar patches based on CHAMP TEC data, Radio Sci., 48, 289–301, doi: 10.1002/rds.20033.

[RD-4] Montenbruck, O. and Kroes, R. (2003), In-flight performance analysis of the CHAMP BlackJack GPS Receiver, GPS Solutions, 7, 74–86, doi: 10.1007/s10291-003-0055-5.

[RD-5] The New Flex Power Mode: From GPS IIR-M and IIF Satellites with Extended Coverage Area, https://insidegnss.com/the-new-flex-power-mode-from-gps-iir-m-and-iif-satellites-with-extended-coverage-area/.

[RD-6] GRACE Payload: K-Band Ranging System (KBR), http://op.gfz-potsdam.de/grace/payload/payload.html.

[RD-7] Yan, Y., Müller, V., Heinzel, G., Zhong, M. (2021), Revisiting the light time correction in gravimetric missions like GRACE and GRACE follow-on, Journal of Geodesy, 95, 48, doi: 10.1007/s00190-021-01498-5.

[RD-8] CEDAR Madrigal Database, http://cedar.openmadrigal.org/.

[RD-9] Bilitza, D., Altadill, D., Truhlik, V., Shubin, V., Galkin, I., Reinisch, B., Huang, X. (2017), International Reference Ionosphere 2016: From ionospheric climate to real-time weather predictions, Space Weather, 15, 418– 429, doi: 10.1002/2016SW001593.

2.3 Abbreviations

A list of acronyms and abbreviations used by Swarm partners can be found here. Some acronyms or abbreviations frequently used in this document can be found below.

Acronym ***or abbreviation***	***Description***
CEDAR	Coupling, Energetics, and Dynamics of Atmospheric Regions
CHAMP	CHAllenging Minisatellite Payload
GPS	Global Positioning System
GNSS	Global Navigational Satellite System
GRACE	Gravity Recovery and Climate Experiment
GRACE-FO	GRACE Follow-On
IRI	International Reference Ionosphere
IRI-2016	International Reference Ionosphere 2016
Ne	electron density
KBR	K-band Ranging
SNR	Signal-to-Noise Ratio
sTEC	slant TEC
RINEX	Receiver INdependent EXchange
TEC	Total Electron Content

Acronym ***or abbreviation***	***Description***
TIRO	Topside Ionosphere Radio Observations from multiple LEO-missions
TMS	time series
vTEC	vertical TEC

3 Algorithms Description

Swarm-TIRO includes two independent groups of products. The first one is Total (topside) Electron Content, which is derived from dual frequency GPS observations and is being processed for each of the five LEO satellite CHAMP, GRACE 1/2, GRACE-FO 1/2 independently. The second one is the local electron density between the GRACE and GRACE-FO satellite duos, which is derived from the dual-frequency inter-satellite KBR measurements. The processing algorithms for each of the product groups are similar for each of the missions and only the input parameters are adjusted for the mission in question. The descriptions of TEC and Ne algorithms are given in sections 3.1 and 3.2, respectively. TIRO utilizes frequency dependent code delay and phase advance of electromagnetic waves in presence of free electrons. Therefore, the information gathered by trans-ionospheric signal propagation contains information about the plasma along the signal path. CHAMP, GRACE, and GRACE-FO are equipped with receivers that are capable of tracking the US-American GPS system on two frequencies. Other GNSS systems exist, such as the European Galileo or the Chinese Beidou among others, but only the TriRO-GNSS receivers onboard the GRACE-FO satellites are multi-GNSS receivers. The amount of non-GPS data is yet limited, thus multi-GNSS was excluded for this project. GRACE and GRACE-FO dual-satellite missions in constellation use an inter-satellite radio link in the Ka-band to precisely measure the inter-satellite distance, which is also affected by the ionospheric electron content between the satellites in a similar way as the GPS signals. The ionospheric information derived from the Ka signals is used to derive the mean electron density between the two satellites, respectively.

3.1 Total Electron Content (TEC)

3.1.1 Mathematical description

Slant TEC (sTEC) is defined as the integrated electron density along the line of sight between a radio transmitter (e.g., GPS satellite) and receiver (e.g., onboard the GRACE-FO satellite). From the frequency dependent signal delays, the line-of-sight sTEC is derived by the following equation:

$$sTEC = \frac{f_1^2 f_2^2}{f_1^2 - f_2^2} \frac{(L_1 - L_2) + \Delta\varepsilon}{K}, \qquad \text{Equation 3-1}$$

where $f_1 (= 1.575{,}42\ \text{MHz})$ and $f_1 (= 1.227{,}6\ \text{MHz})$ are the carrier frequencies, L_1 and L_1 are carrier phase observations in units of meters, and $K \approx 40.3\ m^3 s^{-2}$, and $\Delta\varepsilon$ includes ambiguity parameters and remaining errors, such as differential phase biases and noise in units of meters. The ambiguity parameters included in $\Delta\varepsilon$ are estimated using the code measurements P_1 (L1W) and P_2 (L2W) by computing the mean offset between $L_1 - L_2$ and $P_2 - P_1$ (order of indices different due to the opposite sign in the ionospheric signal content). In contrast to $L_1 - L_2$, $P_2 - P_1$ are not relative measurements, but follow a baseline, which however is still concerned with a satellite intrinsic bias. To make $P_2 - P_1$ fully absolute, the $P_2 - P_1$ differential code biases for the transmitter DCB_T and for the receiver DCB_R have therefore to be applied to $P_2 - P_1$ (see e.g., [RD-3]). sTEC is given in TEC units (TECU) and 1 TECU = $10^{16}\ m^{-2}$. This algorithm to derive TEC is based on an approved method suggested originally in [RD-1] [RD-2] that has been adapted to process signals received at LEO-satellites. Applying an appropriate mapping function maps the line-of-sight sTEC into vertical TEC (vTEC) and is described in [RD-3].

The algorithm applied here to derive relative and absolute sTEC and mapping it to absolute vTEC is similar to the one that is operationally applied in the processor implemented for Swarm and a detailed algorithm

description is given in [AD-3]. The general description of the processing flow[1] of the Swarm TEC algorithm is presented in 3.1.2. Parts of those modules that needed to be adapted or improved for the CHAMP, GRACE or GRACE-FO missions are described in more details in subsections of 3.1.2.

3.1.2 Processing overview

The TEC product is derived daily upon the availability of all input data. The processing flow of the algorithm for Swarm TEC consists of eight main modules described below. The high-quality dual-frequency phase observations are used to derive TEC in the processor. They may be affected by cycle slips and in order to obtain an absolute value the remaining phase ambiguity has to be estimated. This is performed using the cycle slip and ambiguity-free code observations. Modules 2 and 3 are used twice because further cycle slip correction and outlier detection may apply to multipath cleaned observations (steps 5 and 6, respectively)

1. Module 1: Preparation of input data (section 3.1.2.1)
    a. Setting of configuration parameters
    b. Processing period determination
    c. Input data identification and preparation
2. Module 2: Cycle-slip detection (section 3.1.2.2)
    a. Creating wide lane combinations from GPS phase observables
    b. Iterative wide lane average and standard deviation calculation
    c. Outlier detection and elimination and replacing eliminated data point by interpolation
    d. Identification of cycle slips
    e. Definition of preliminary connected arcs
3. Module 3: Cycle-slip correction (section 3.1.2.3)
    a. Spline/Polynomial extrapolation of consecutive arcs
    b. Cycle-slip correction, if noise level is sufficiently small
    c. Generation of final, longer connected arcs
4. Module 4: Multipath estimation and correction (section 3.1.2.4)
    a. Estimation of multi-path effects in the code phase
    b. Correction of multi-path effects in the code phase
5. Module 2: Cycle-slip detection
6. Module 3: Cycle-slip correction
7. Module 5: Calculation of relative slant TEC (section 3.1.2.5)
    a. Estimation of the remaining ambiguity term using the code measurements
    b. Calculation of relative slant TEC
    c. Calculation of the RMS between code-phase and code-levelled carrier-phase TEC for uncertainty estimation of the levelling in 7.a
    d. Reordering GPS arc-related observations by time

[1] The module names and text description presented here can differ from [AD-3].

8. Module 6: Estimating differential code bias of the GPS receiver (section 3.1.2.6)
    a. Calculation of differential code bias of the receiver
    b. Validation of differential code bias of the receiver
    c. Calculation of the uncertainty of the receiver differential code bias estimate
9. Module 7: Calculation of absolute slant and absolute vertical TEC (section 3.1.2.7)
    a. Calculation of absolute slant TEC
    b. Calculation of absolute vertical TEC
10. Module 8: Output (section 3.1.2.8)
    a. Create CDF output of the TEC processing results

3.1.2.1 *Module 1: Preparation of input data*

The preparation of the input data is mainly unmodified to the module applied for Swarm. The input data of the current day are processed daily including, if available, an overlap up to one hour with the previous and the next day to avoid discontinuities. If the input data of the previous or following day is not available, only the data of the current day is used. If the input data of the current day is not available, then the TEC processing for the current day is skipped. The required input data products are listed below for each mission [AD-2]. These are:

CHAMP:
GPS satellite ephemeris (CODwwwwd.EPH) and transmitter biases (CODGddd0.yy), CHAMP satellite position (CH-OG-3-RSO+CTS-CHA_yyyy_ddd_hh.dat) and GPS observation data (CH-OG-1-SST+yyyy_ddd_00_x.v.rnx).

GRACE:
GPS satellite ephemeris (CODwwwwd.EPH) and transmitter biases (CODGddd0.yy), GRACE 1 and 2 satellite positions (GNV1B_yyyy-mm-dd_n_02.dat) and GPS observation data (GPS1B_yyyy-mm-dd_n_02.rnx).

GRACE-FO:
GPS satellite ephemeris (CODwwwwd.EPH) and transmitter biases (CODGddd0.yy), GRACE-FO 1 and 2 satellite positions (GNV1B_yyyy-mm-dd_n_04.dat) and GPS observation data (GPS1B_yyyy-mm-dd_n_04.rnx).

3.1.2.2 *Module 2: Cycle-slip and outlier detection*

The cycle slip detection module is similar to the one described for the Swarm processor, but with the following updates for all three missions CHAMP, GRACE and GRACE-FO:

- The elevation angle filter to deselect GPS observations with a ray elevation angle less than 20° from processing is removed
- Instead, a new filter based on the GPS signal-to-noise ratio (SNR), S_1 and S_2, is implemented. S_1 and S_2 (measured on $L1C$ and $L2W$) are therefore translated to C_1/N_0 and C_2/N_0, where $C/N_0 = 20\ \log_{10}(S/\sqrt{2})$ [RD-4]
- For cases, where C_1/N_0 or C_2/N_0 is smaller than 23.01 dB-Hz, the observations are removed

- The ratio of C_2/N_0 and C_1/N_0 is checked to screen for tracking issues. For CHAMP a lower threshold of 0.7 and an upper threshold of 1.8 is selected. For GRACE only the lower threshold of 0.7 had to be applied
- The minimal arc length is increased from 9 data points to 20 for the updated version, which correspond to 200-second-long arc for the 1/10 Hz sampling rate of CHAMP, GRACE, and GRACE-FO
- The value of the standard deviation (σ) of the Melbourne-Wuebbena linear combination of carrier phase observations that is used to detect cycle slips is set to a constant value of 0.43 m, e.g., it is not iteratively adapted
- Outlier interpolation of data points at times of eliminated outliers is deactivated and instead, the following conditions are used
    - The original data point is kept if its magnitude in the linear combination of the carrier phase observation is less than 4 times the standard deviation ($4 \cdot \sigma$)
    - otherwise, the data point is discarded and no interpolation is performed, which then result in a data gap at this respective time stamp

3.1.2.3 *Module 3: Cycle-slip correction*

There are no modifications in this module compared to the one implemented for Swarm [AD-3].

3.1.2.4 *Module 4: Multipath estimation and correction*

There are no modifications in this module compared to the one implemented for Swarm [AD-3].

3.1.2.5 *Module 5: Calculation of relative slant TEC*

There are minor modifications in this module for GRACE-FO compared to the one implemented for Swarm [AD-3]. In order to account for tracking issues regarding flex power. For that purpose, the arc-wise median value of each arc is computed. For each PRN the median over all arcs is valuated and arcs whose median differs more than 50 TECU are rejected.

3.1.2.6 *Module 6: Estimating differential code bias of the GPS receiver*

There are minor modifications in this module compared to the one implemented for Swarm [AD-3]. The DCB vertical limit to form pairs for DCB estimation was increased from 3 TECU to 10 TECU to ensure enough pairs for robust receiver DCB estimation.

3.1.2.7 *Module 7: Calculation of absolute slant and absolute vertical TEC*

There are no modifications in this module compared to the one implemented for Swarm [AD-3].

3.1.2.8 *Module 8: Output*

The output product files are in CDF and aligned in format with the Swarm Level 2 TEC product files. Few modifications have been applied for all three CHAMP, GRACE and GRACE-FO missions:

- The S_1 signal to noise ratio translated to C_1/N_0 for $L1C$ is added (see section 3.1.2.2)
- The S_2 signal to noise ratio translated to C_2/N_0 for $L2W$ is added (see section 3.1.2.2)

The complete TEC product file format for CHAMP, GRACE and GRACE-FO missions and their format are described in [AD-2].

3.1.3 Details for Flex Power regarded updates

The recently enabled Flex Power mode [RD-5] heavily affects observations at the GPS receiver's tracking onboard the GRACE-FO satellites. Flex Power is redistributing the output power between the transmitted signals of the GPS satellites if the GPS satellite is inside a specific region. During Flex Power mode II and IV the GRACE-FO TriRo-GPS receiver encounters serious tracking issues in $L1C$ and $L2W$. An updated version of the algorithm to handle periods of Flex Power issues is currently implemented. To circumvent disturbances due to Flex Power mode will be the identification arc wise median of relative TEC is tested. If the median of an arc differs more than 50 TECU from the median of all arcs of that specific PRN the arc is removed. To minimize false rejections, this test is only performed for Flex Power active periods when the ratio $S_1/S_2 > 1.1$ and eliminate these data the respective satellite is capable of Flex Power. Such tracking issues connected to Flex Power were not observed for the Swarm GPS receiver, however, minor changes in the GPS satellite's DCB should be accounted for are observed.

3.2 Electron density (Ne) derived from KBR

3.2.1 Mathematical description

The GRACE and the GRACE-FO missions consist each of two identical spacecraft following each other with about 220 km distance on the same orbital track. The missions aim primarily to measure the Earth's gravity field and its time variability with unprecedented accuracy. The twin spacecraft are interconnected by a K-Band ranging (KBR) system, using microwaves at K ($f_K = 24$ GHz) and Ka ($f_{Ka} = 32$ GHz) frequencies to measure the relative distance between the twin satellites and its rate of change with an accuracy of better than $0.1\ \mu m\ /\ s$ for both satellite missions ([RD-6] and [RD-7]). In a first approximation, the phase measurement L_i (L_K and L_{Ka}) on frequency f_i (f_K and f_{Ka}) in meters can be decomposed as

$$L_i = \rho - I_i + \delta c + \lambda_i n_i, \qquad \text{Equation 3-2}$$

where ρ is the geometric range, I_i is the frequency dependent ionospheric delay in units of meters (note the sign, thus the phase advances), δ contains the clock corrections in seconds and c is the speed of light in m/s. The wavelength is λ_i and n_i (unitless) denotes the ambiguity parameter. The ionospheric component I_i can to first order be expressed as

$$I_i = \frac{1}{f_i^2}\frac{1}{2}\int_t^r f_p^2 dl = \frac{1}{f_i^2}\, K \int_t^r N_e dl = \frac{1}{f_i^2}\, K\, TEC, \qquad \text{Equation 3-3}$$

where f_p is the plasma-frequency which is integrated along the line-of-sight between transmitter t and receiver r. The plasma density is denoted as N_e and the Total Electron Content as TEC. The constant $K \approx 40.3\ m^3 s^{-2}$ is identical to the constant used for TEC processing (section 3.1.1). By appropriate combinations of the phase observations at the two frequencies available, either the ionospheric component, I_i, is eliminated, or range correction (e.g., phase center offset) and receiver/transmitter clock corrections, δ, are removed. The ambiguity term remains in each approach. In the case of GRACE and GRACE-FO, the relative TEC, $rTEC$, in units of m^{-2} can be computed from $Iono_{Corr}$ ([AD-4], page 21, section 4.1.3) by

$$rTEC = Iono_{corr} \cdot \frac{f_{Ka}^2}{K}. \qquad \text{Equation 3-4}$$

Here f_{Ka} is the Ka frequency of 32 GHz. It should be noted that Equation 3-4 only provides a relative value since the phase ambiguity parameter for these KBR observations is unknown. However, this ambiguity parameter can be assumed to be constant, as long as no phase break occurs. When dividing $rTEC$ (in TECU) by the geometric distance of the satellite pair, one can obtain an estimate of the mean relative electron density, rN_e, in m^{-3} between both satellites

$$rN_e \approx \frac{rTEC}{d} \qquad \text{Equation 3-5}$$

where d is the distance between the two satellites. For absolute levelling of the relative electron density, external information is required. Here the IRI-2016 model is used to estimate the required shift for levelling to eliminate the ambiguities.

3.2.2 Technical implementation overview

The peculiarity of the KBR N_e processing is the handling of daily available data which are organized in arcs that can have a length of several minutes up to months. This information is unknown at the beginning thus the available files need to be screened and arcs need to be identified. Full arcs are required to ensure consistent levelling. Thus, it is necessary to collect data until the current arc is completed, which can take up to a few months.

For these reasons, processing the final daily N_e files from KBR data needs some prior information, which requires partly processing the same data in multiple rounds and is described later in this section. This prior information is:

1. Identify start and end time of each arc.
2. Identify time and magnitude of any discontinuity at a day-to-day UT boundary, e.g., at 00UT (inconsistency of levelling in the input files).
3. Levelling of the first value of $Iono_{Corr}$ of an arc to zero (to avoid numerical issues when deriving relative N_e).
4. Identify intervals of data to be excluded due to outliers.
5. Model calibration data.

3.2.3 Processing overview

The N_e product CDF files will be provided as daily files and those are derived in patches once in a 3-4 months period and upon the availability of all input data including the calibration data, e.g., radar or IRI model values. The processing flow of the algorithm for GRACE and GRACE-FO consists of five main modules:

1. Module 1: Identify a continuous arc (section 3.2.3.1)
    a. Read daily KBR files
    b. Identify discontinuities, such as artificial jumps at arc offsets at UT-day boundaries
    c. Create internal output file **01_offset.dat** including marker, time, and amplitude of the jumps
2. Module 2: Derive preliminary relative N_e (section 3.2.3.2)
    a. Read daily KBR, GNV1B (satellite 1) and GNV1B (satellite 2) files
    b. Read internal 01-offset.dat file
    c. Derive preliminary relative N_e based on Equation 3-4 and Equation 3-5

   d. Create daily internal intermediate output files **02_prel_rel_density.dat**

3. Module 3: Screen daily files of preliminary relative N_e for outliers (section 3.2.3.3)
   a. Read internal 01_offset.dat and 02_prel_rel_density.dat files
   b. Identify problematic observations of preliminary relative N_e that are rejected if at least one of the six criteria described in section 3.2.3.3 applies to the observation. These are then identified as outliers and will be discarded in modules 4 and 5.
   c. Create internal output file **03_outlier.dat**
4. Module 4: Prepare calibration based on model data (section 3.2.3.4)
   a. Read daily 02_prel_rel_density.dat and 03_outlier.dat files
   b. Read model (IRI-2016) and determine the offset between relative Ne and model data
   c. Create internal output file **04_calib_iri.dat** including the identified offsets
5. Module 5: Output (section 3.2.3.5)
   a. Read daily KBR, GNV1B (satellite 1) and GNV1B (satellite 2) files
   b. Read internal output 01_offset.dat, 03_outlier.dat, 04_calib_iri.dat files
   c. Calculate relative N_e
   d. Use 04_calib_iri.dat files and calculate absolute N_e by applying the identified offset. If no calibration offset for the specific arc exists in 04_calib_iri.dat files, the variable "absolute N_e" is set to NaN
   e. Create **daily CDF output** files of KBR N_e processing results

3.2.3.1 *Module 1: Identify continuous arcs*

At first step, continuous arcs are identified in the GRACE-FO (GRACE) satellite data time series of the KBR Level 1B daily files. There often exist discontinuities, e.g., jumps in the time series mainly connected to data gaps in $Iono_{Corr}$ or to the transition between the KBR Level 1B daily files, e.g., near 00UT of 2018/05/30 (Figure 3.2-1). To identify and possibly correct for jumps between arcs, the following procedure is applied and a bias describing the amplitude of the jump is derived to be applied to $Iono_{Corr}$ for the specific day and arc.

A new arc is identified if one of the following conditions are satisfied:

1. the phase break flag is set in the original KBR-file;
2. a gap of more than 7.5 seconds between two subsequent observations occurs (the regular sampling is 5 s);
3. the absolute difference of two subsequent $Iono_{Corr}$ values is larger than 0.02 m.

Possible jumps near the UT-day boundary in the absence of a data gap are checked for and corrected as following:

1. the last 5 observations of a daily file and the first 5 observations of the following daily file are within 50 seconds; thus, data is complete (5 s sampling, no gap);
2. fit a linear polynomial to the last 5 observations of the following daily file and extrapolate for the next value, compute the difference between extrapolated value and observed value, δ_{left};
3. fit a linear polynomial to the first 5 observations and extrapolate for the previous value, compute the difference between extrapolated value and observed value, δ_{right};
4. derive $\delta = (\delta_{left} - \delta_{right})/2$;

5. update bias $bias_{updated} = bias_{previous} + \delta$.

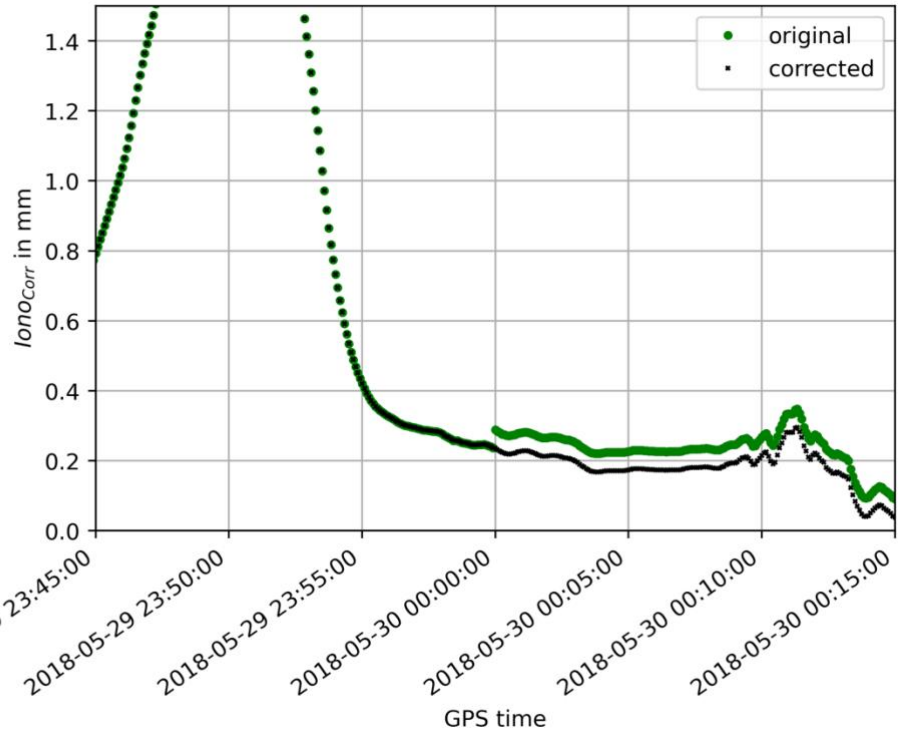

Figure 3.2-1 Discontinuity correction performed on $Iono_{Corr}$ (black: corrected; green: original) near the day boundary at 00UT of 2018/05/30.

The results are stored in the internal file **01_offset.dat**, that contains the variable $bias_{updated}$ derived in point 5 (see here above), the epoch, from which on this bias is valid, the first value of the new arc, and a flag, if a new arc starts (flag is set to 1), or if only a step at the near-inter-day boundary was corrected (flag is set to 0). The first $Iono_{Corr}$ value of each arc is stored since it is later subtracted before the computation of relative N_e, because numerical issues were observed, if the jumps between the arcs are very large in magnitude.

The content of **01_offset.dat** contains step corrections for daily KBR files and offsets for each arc.

3.2.3.2 *Module 2: Derive preliminary relative N_e*

The preliminary N_e is computed from the daily KBR, GNV1B (satellite 1) and GNV1B (satellite 2) files and from information in 01_offset.dat. Now, each arc of $Iono_{Corr}$ is shifted, such that the first value of the arc equals 0. This is, in theory, irrelevant, since the magnitudes of the data are still ambiguous to an unknown value. However, dealing with too large values of $Iono_{Corr}$, resulted in numerical annihilation when dividing two float64 numbers, which is required for solving Equation 3-6. After computing the geometrical distance between the satellites, d, at each observation datum, the preliminary relative electron density, rN_e (in m^{-3}), is derived as

$$rN_e = \frac{1}{d}\frac{\left(Iono_{corr} - b(t)\right)\cdot f_{Ka}^2}{K}. \qquad \text{Equation 3-6}$$

In this equation, $b(t)$ is the bias (in meters, see module 1 in section 3.2.3.1) valid at epoch t. By applying this bias no discontinuities occur anymore near the UT-day boundaries. The position of the estimated local electron density is the geometric mean of the positions of the two GRACE-FO (GRACE) satellites.

The results are stored in the internal file, **02_prel_rel_density.dat**. The file 02_prel_rel_density.dat contains the epoch, the geographic and magnetic coordinates (QD latitude and MLT) of the local electron density estimate, the satellite 1 and 2 positions, $Iono_{Corr}$, the distance between satellites 1 and 2, the relative horizontal TEC, and the preliminary relative density.

3.2.3.3 *Module 3: Screen daily files of* preliminary relative N_e

To account for the occasional occurrence of unrealistic large variations within one arc of electron density values and of degradations near the start or end of an arc, the following criteria were used to identify problematic observations to be rejected:

1. If the difference between maximum rN_e and minimum rN_e exceeds $2 \cdot 10^{12}/m^3$ the full arc shall be rejected.
2. If the difference between maximum rN_e and minimum rN_e during the first 20 observations exceeds $1 \cdot 10^{11}/m^3$ the first 20 observations shall be rejected.
3. If the difference between maximum rN_e and minimum rN_e during the last 20 observations exceeds $1 \cdot 10^{11}/m^3$ the last 20 observations shall be rejected.
4. If the correlation coefficient to a fitted sinus curve is above 0.9 the whole arc shall be rejected.
5. Short excursions, which are $1 \cdot 10^{11}/m^3$ lower than the 0.05 quantile of the arc ($\pm$ 30 s) shall be rejected.
6. Arcs which have a poor correlation to the IRI model (less than 0.65, Pearson) shall be rejected.

The results are stored in the internal file, **03_outlier.dat**. It contains the time spans in cdf-epoch where the observations are to be rejected including its reason as given above.

3.2.3.4 *Module 4: Calibration model data*

The preliminary satellite electron density is calibrated against an empirical model, e.g., the IRI-2016 model (state of 02/22/2022, code frozen, only coefficients updated) [RD-9]. Modelled electron density is computed for each observation of relative electron density that was not identified as an outlier or included in unreasonable disturbed periods. For each connected arc, the mean offset between the relative N_e (rN_e) and the electron density provided by IRI-2016 N_{eIRI} (both in $1/m^3$) is computed (Figure 3.2-2) using

$$b_{IRI} = \frac{1}{n_{obs}} \sum_{i=1}^{n_{obs}} rN_e(t_i) - N_{eIRI}(t_i). \qquad \text{Equation 3-7}$$

The mean offset to IRI-2016 determined electron density for each arc is stored in the internal file, **04_calib_iri.dat**.

In earlier versions, radar calibration was considered but this was rejected due to large uncertainties in altitudes of 400 km to 600 km, especially for the near-polar EISCAT stations and the large number of arcs left uncalibrated due to missing conjunctions. Radars were considered for validation purposes only.

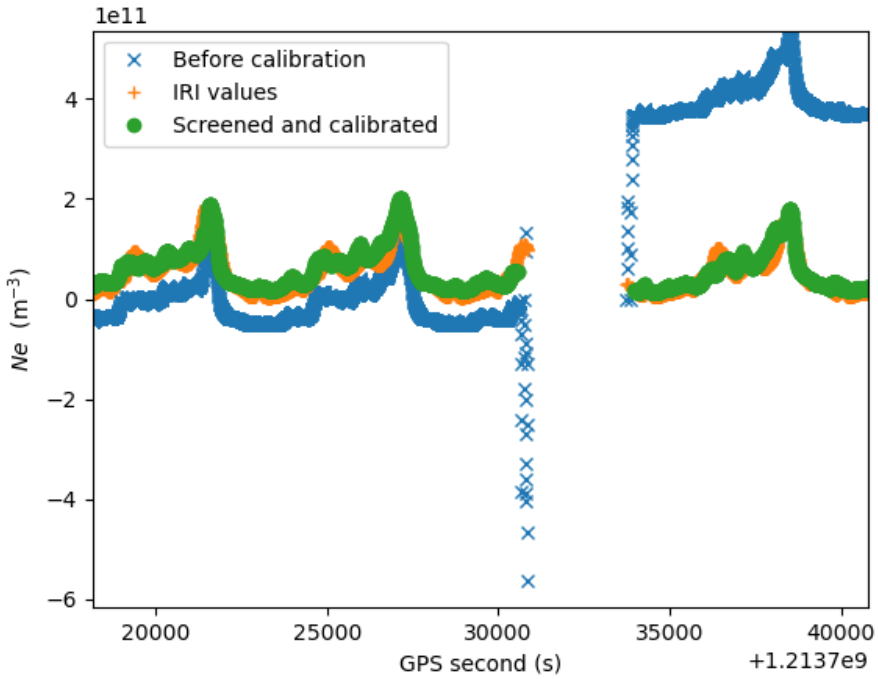

Figure 3.2-2 Preliminary N_e (blue), IRI-2016 N_e values(orange), and screened and calibrated N_e values (green).

3.2.3.5 *Module 5: Output*

All steps that were performed in modules from 1 to 4 allow calculating absolute N_e based on the original input data for one continuous arc (note: an arc can span a time between few minutes and several months), and create the daily output CDF files.

The final cdf data is created using IRI-2016 calibration data, **04_calib_iri.dat**,

$$aN_e = rN_e - b_{IRI} \text{ (see Equation 3-7).} \qquad \text{Equation 3-8}$$

Daily CDF output files are described in detail in [AD-2]. The release of the output is realised in batches of a few months, which give an opportunity to calibrate newly recorded GRACE-FO data. The GRACE data are available for the entire completed mission duration. Furthermore, the updates of the IRI coefficient files are required, which are published every 6 months.

4 Summary and conclusions

This document described the processing algorithm to derive TEC from GPS observables at CHAMP, GRACE, and GRACE-FO, and to derive in situ electron density derive from Ka-band observations between the twin satellites of GRACE and GRACE-FO.

The document [AD-5] (validation report) will describe the assessment of the results.